

Mikroskopické techniky v Ramanově spektroskopii

Vladimír Baumruk

Fyzikální ústav UK



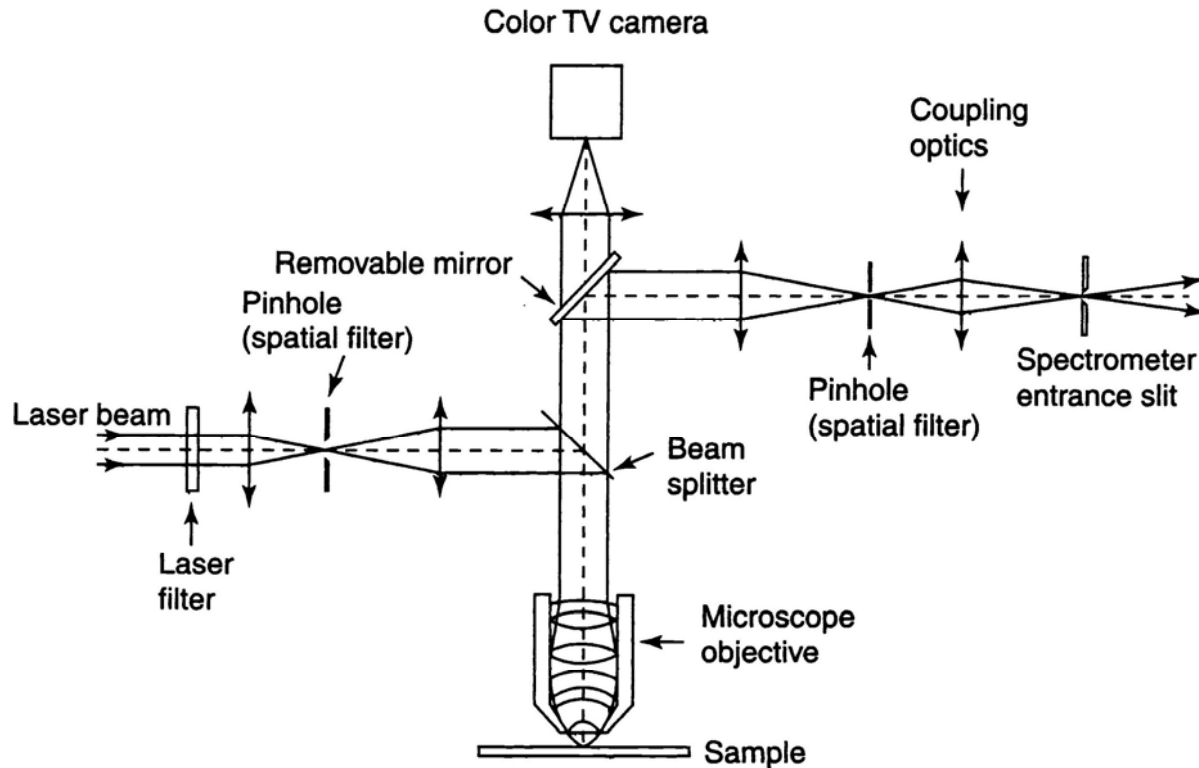
PROČ ?

- vysoké prostorové rozlišení v ploše (rovina XY) a v případě konfokálních systémů i v hloubce

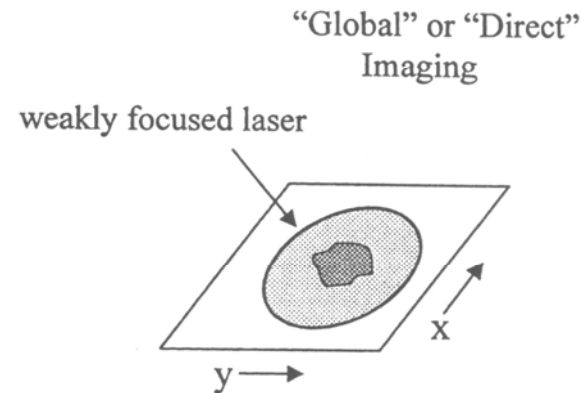
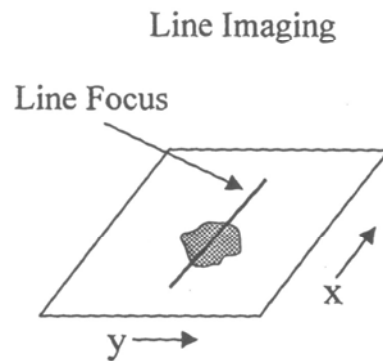
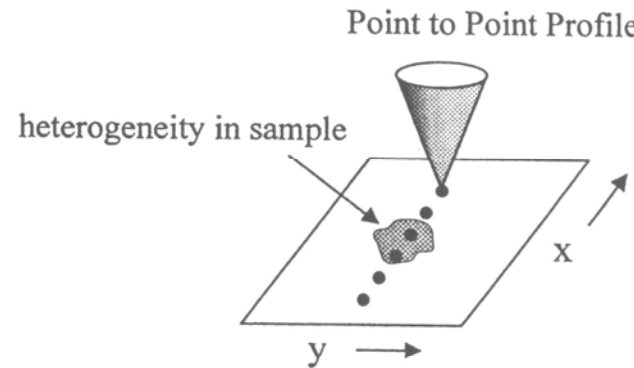
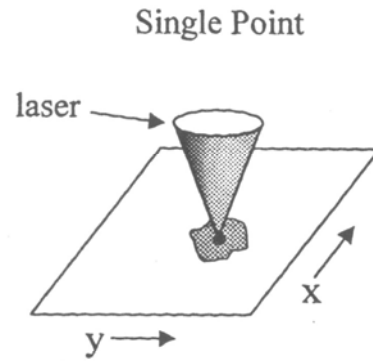
VÝHODY

- při vysoké numerické apertuře v geometrii zpětného rozptylu (180°) je dodatečnou výhodou široký kónus sběru rozptýleného záření
- při zobrazení malé stopy budícího svazku na vstupní štěrbinu monochromátoru lze dosáhnout toho, že při vstupních šterbinách $100\ \mu\text{m}$ a větších analyzujeme prakticky veškeré sebrané záření

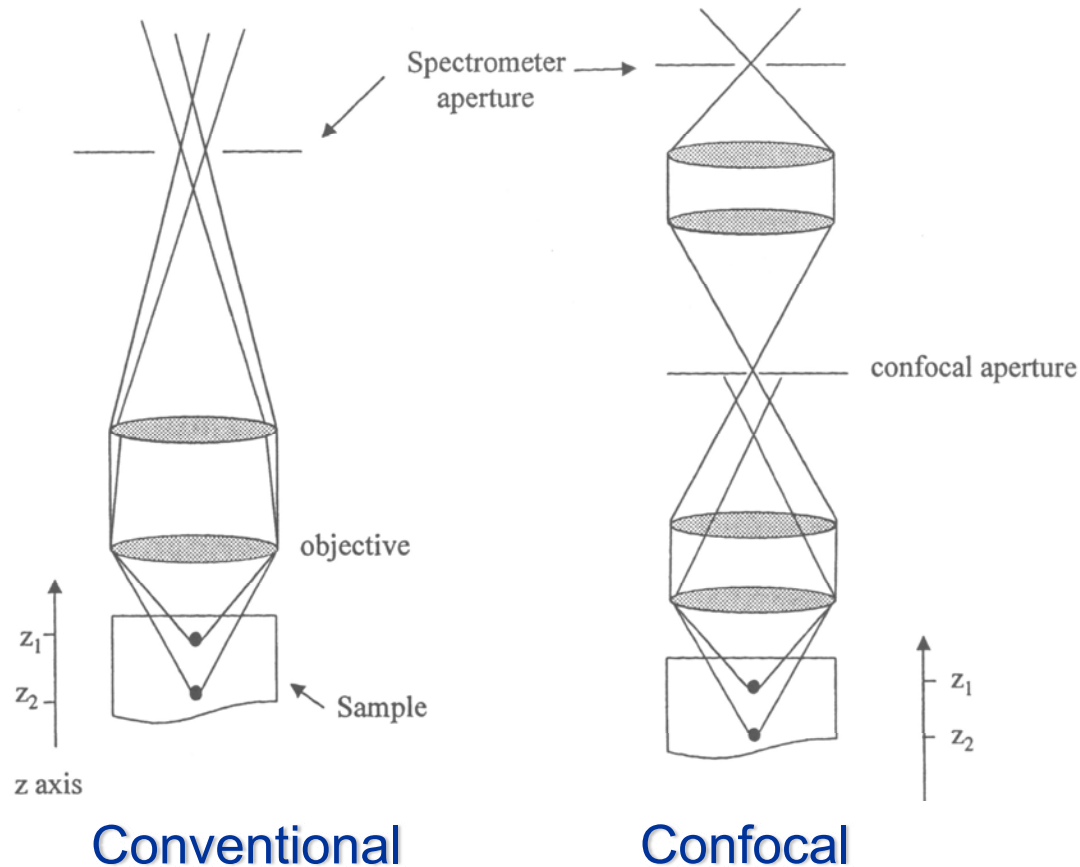
Optical scheme of the widely adopted illuminating and collecting optics for micro-Raman spectrometer



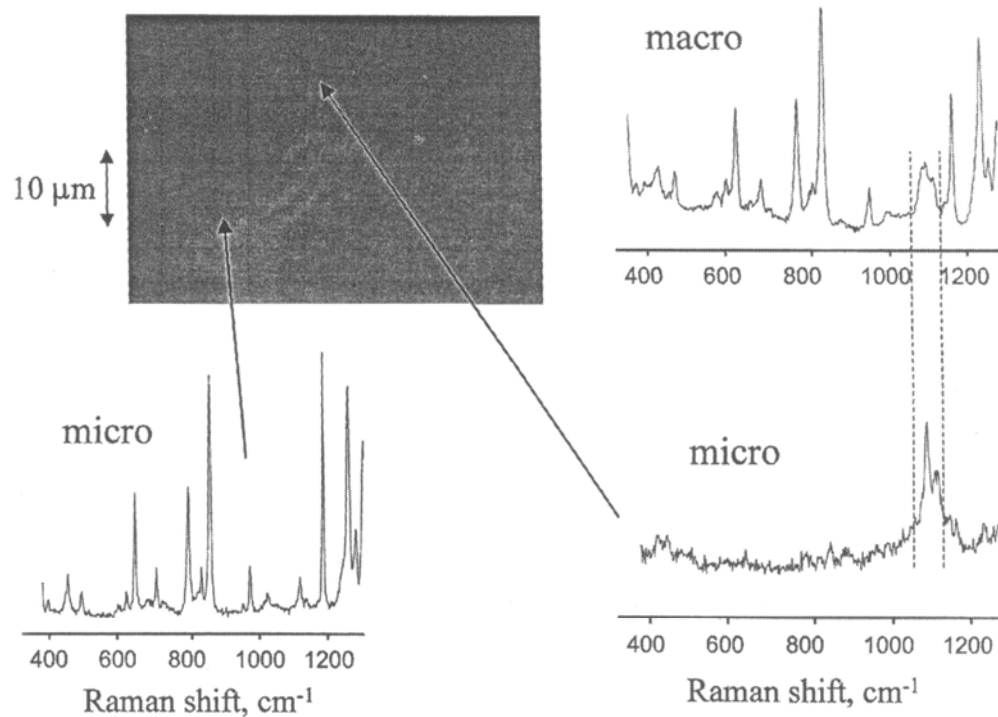
Imaging modes for Raman microscopy



Schematic of confocal microscopy optics, showing addition of a „confocal aperture“ that restricts sampling depth

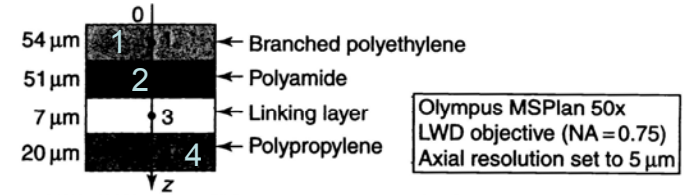
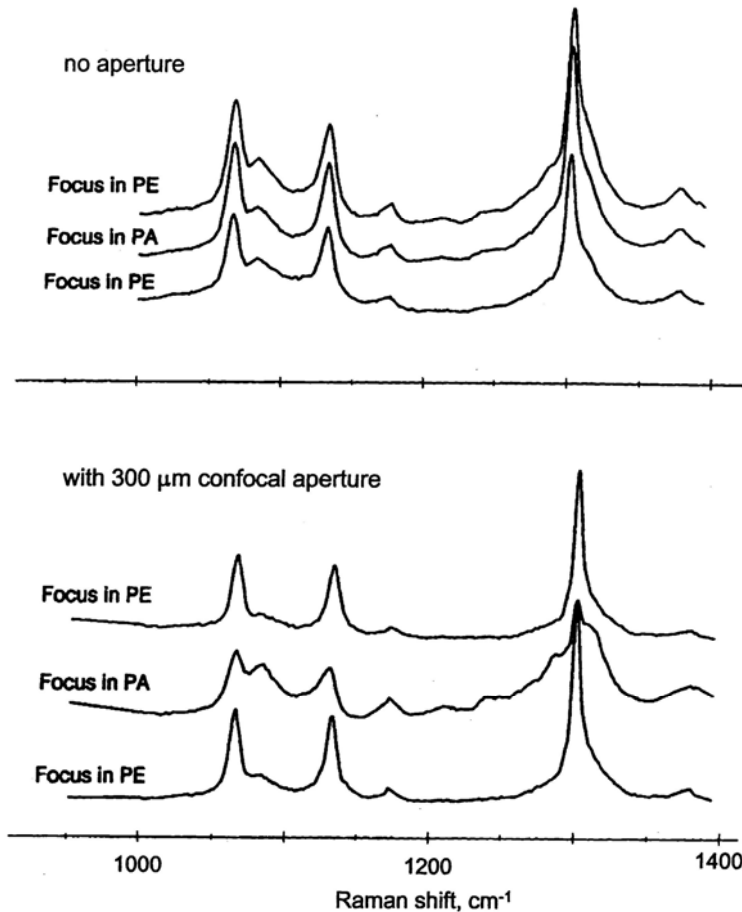


Single point Raman microspectroscopy

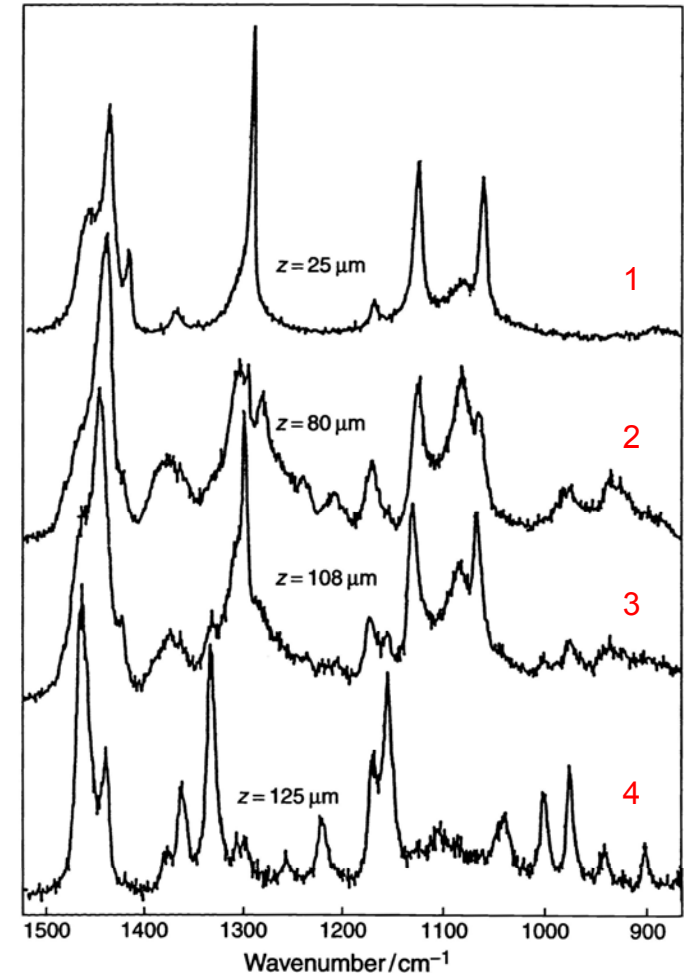


Single point Raman microspectroscopy of a pressed tablet containing acetamidophenol and microcrystalline cellulose. The macro was obtained with an $\sim 100 \mu\text{m}$ -diameter sampling area, and the micro spectra were obtained at the locations indicated.

Depth discrimination in Raman microspectroscopy

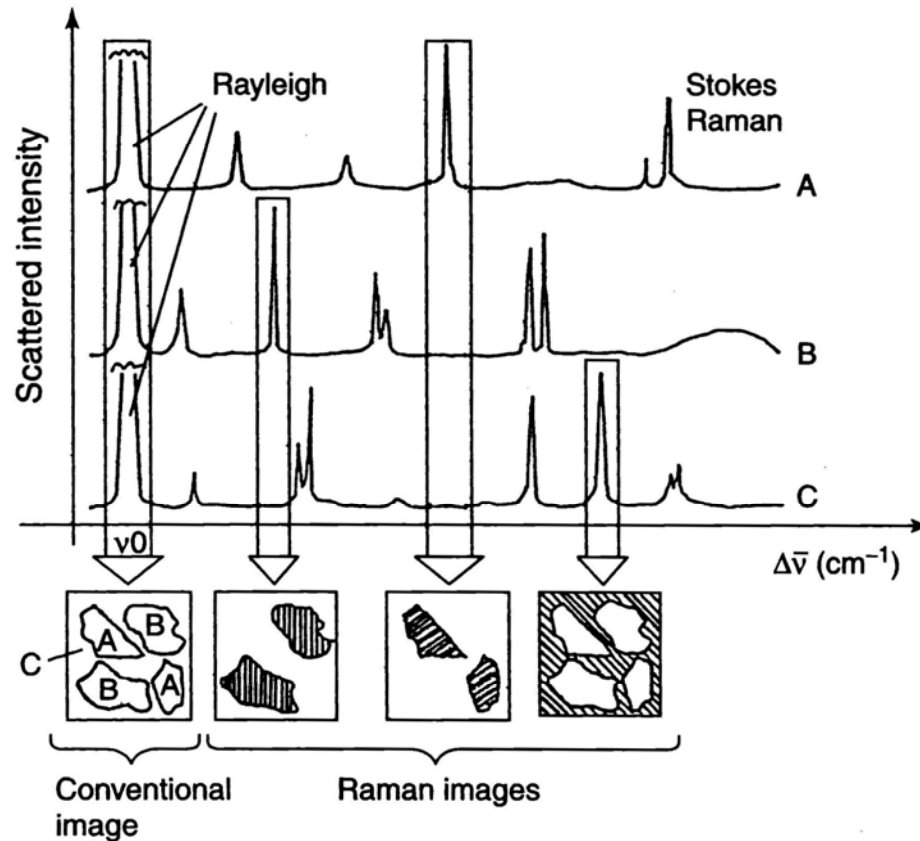


Olympus MSPlan 50x
LWD objective (NA = 0.75)
Axial resolution set to 5 μm



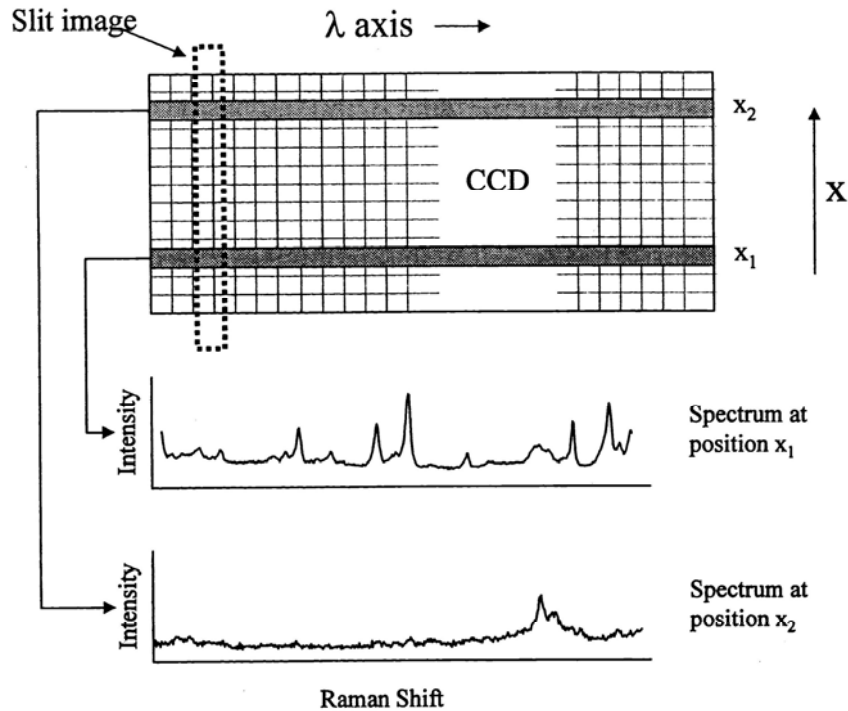
Depth analysis of a multilayered laminate polymer.

Principle of Raman mapping

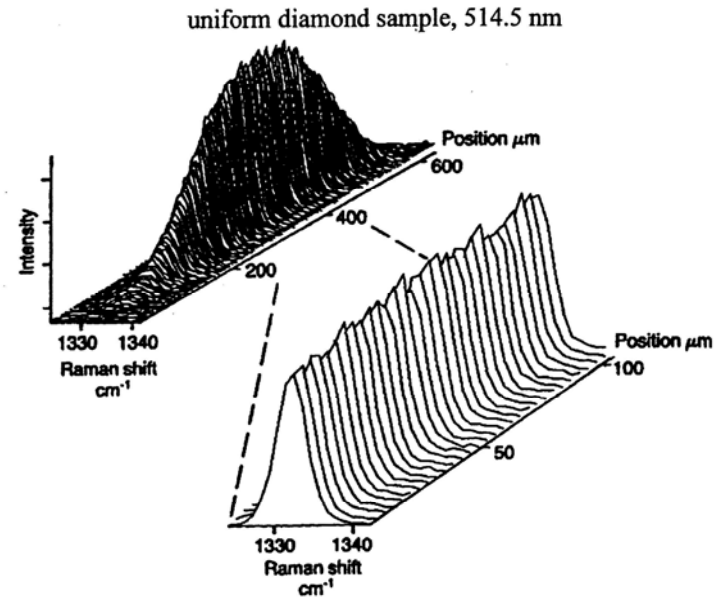


Selective maps of the sample depicting the distribution of a given molecular species can be obtained by passing the Raman scattered radiation through the spectrograph, acting as a narrow-band optical filter, which isolates a narrow spectral region centered on a characteristic Raman wavenumber of this species.

Line imaging



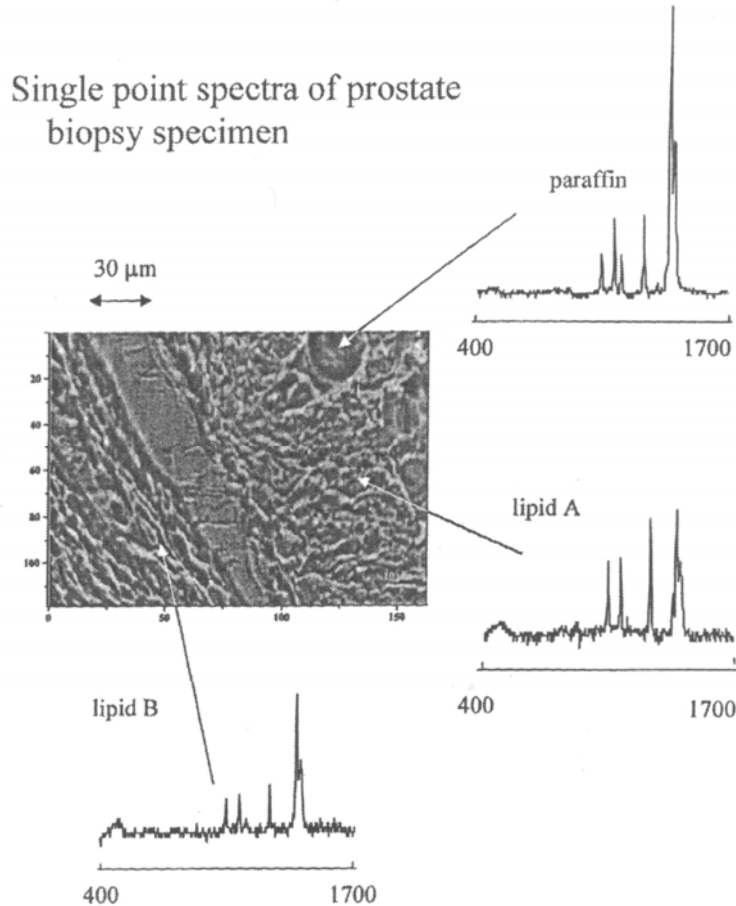
Schematic of line imaging onto a CCD. A line focus at the sample projected onto the slit of an imaging spectrograph generates a 2D image of intensity vs. x and $\Delta\tilde{\nu}$.



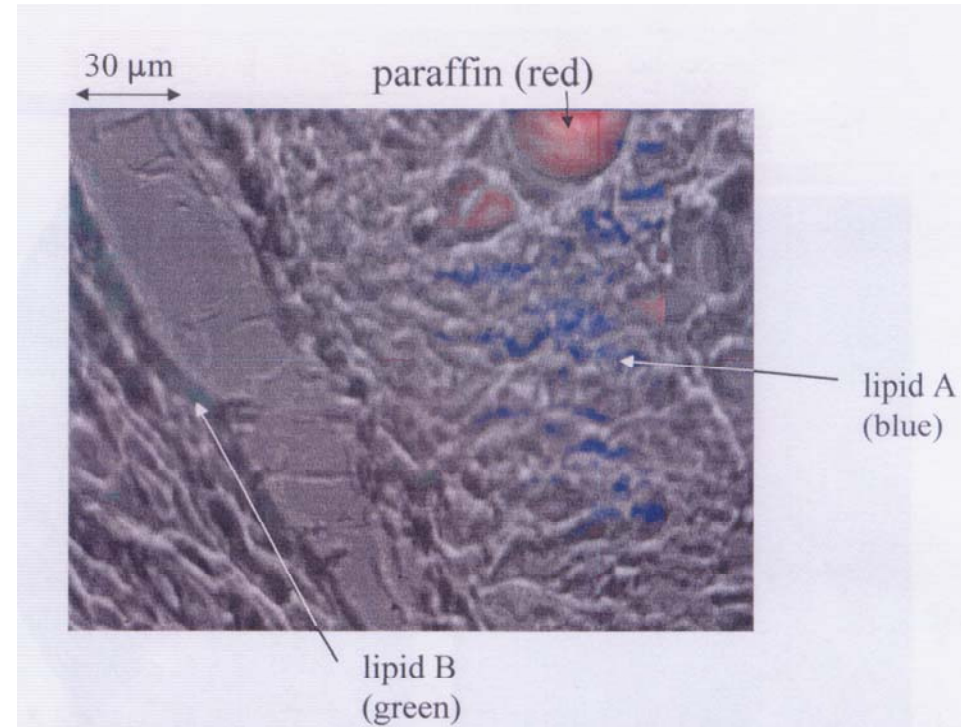
200 Raman spectra of the 1332 cm^{-1} feature of diamond obtained with a $600 \mu\text{m}$ long line focus. The expansion of the middle $100 \mu\text{m}$ of the line demonstrates relatively constant laser intensity.

2D-Raman imaging

Data analysis techniques based on chemometrics and factor analysis may be applied to large spectral data sets to provide greater chemical selectivity. Instead of observing distribution of **a particular Raman band**, the distribution of **an entire spectrum** is determined.

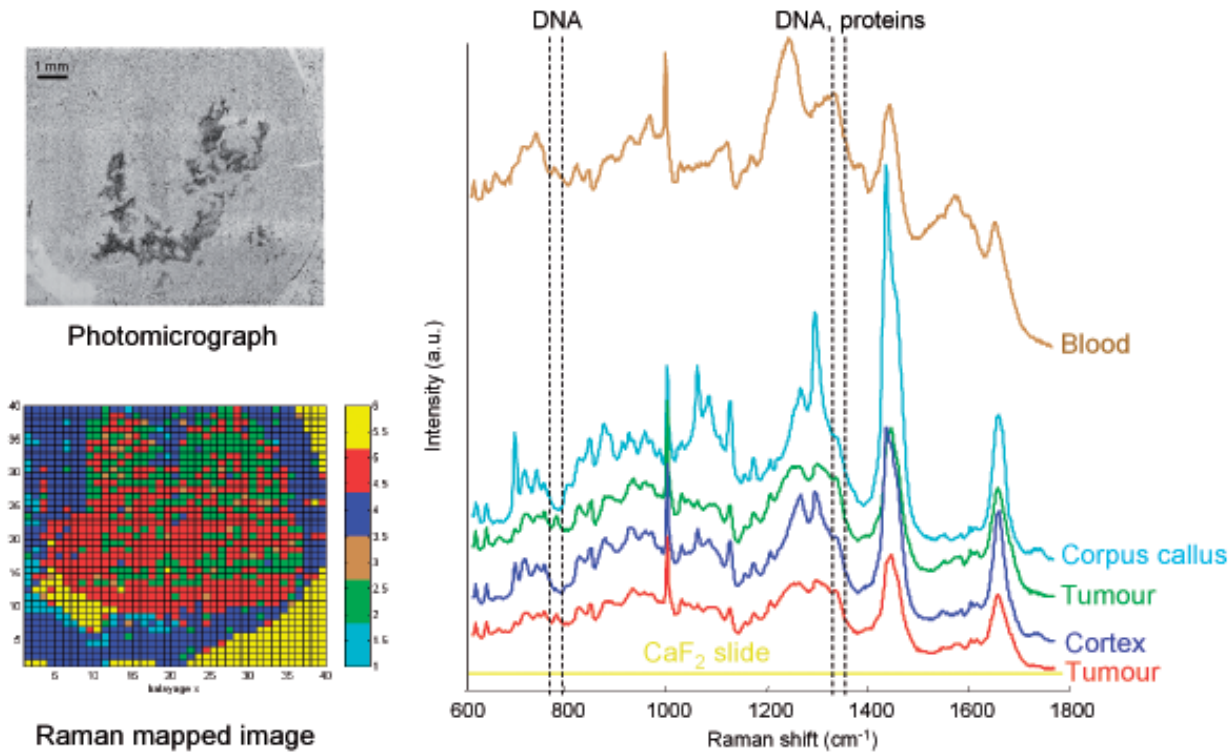


Raman microspectroscopy of a human tissue slice from a prostate cancer biopsy specimen mounted in paraffin.



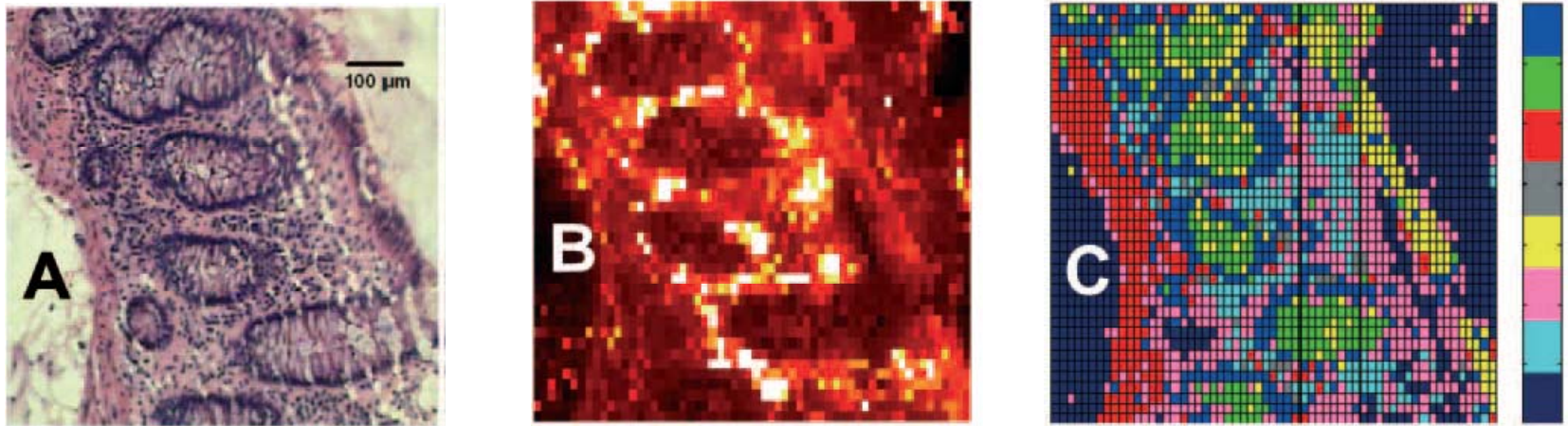
Distribution of components overlaid on the video image. Each color represents the contribution of a particular component to the Raman spectrum observed at each position of a 28 x 28 grid.

Results from mapped imaging of an unstained rat brain tissue section



Photomicrograph and Raman mapped image of a rat brain tissue section, with coloured regions corresponding to the offset spectra shown on the right. Different tissue types are shown in the pseudo-colour Raman map, corresponding to both healthy (corpus callus, cortex, and blood) and diseased (tumoral) tissue. The red tumoral zone correlates directly to histopathological observations with H/E staining.

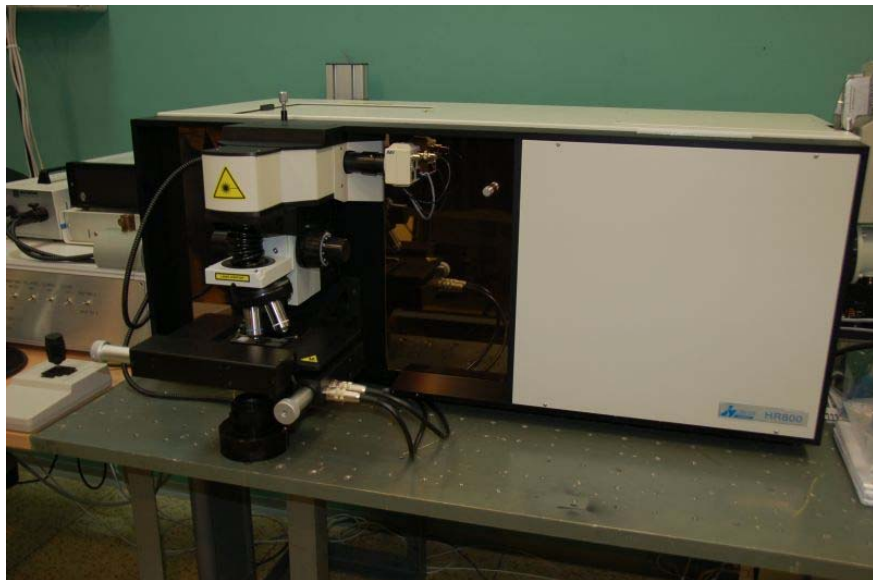
Raman (chemical) imaging



Analysis results for human colonic tissue section (A) optical image of histopathologic HE stained tissue, (B) Raman mapped image illustrating intensity of the Amide I band, and (C) pseudo-colour Raman maps created by using K-means cluster analysis in which each cluster (consisting of similar spectra) is assigned to one color.

It is immediately clear that the visible structural features of the tissue coincide with the chemical information provided by the Raman. Cluster analysis of the Raman data allows spectra of similar profile to be grouped and displayed as a single unit, allowing specific tissue types to be located. This technique makes use of the large information content present even in just one spectrum, which will give an indication of the presence of the various chemicals present within the tissue, such as DNA, RNA, protein, lipid and carbohydrate.

LabRam HR (Horiba Jobin Yvon)



verze VIS (400 - 1100 nm)
ohnisková vzdálenost 800 mm, flat field
2 mřížky 600 a 1800 vrypů/mm
LN2 chlazený CCD detektor 1024x256 pixelů
excitace He-Ne laser 633 nm (interní)
vzduchem chlazený Ar⁺ 514.5, 488 nm (externí)
laserová dioda 785 nm (externí)

konfokální mikroskop Olympus BX41 (open)
motorizovaný XY stolek, krok 0.1 μm
hloubkové profilování rozsah 80 μm , krok 0.1 μm
optika pro pozorování v polarizovaném světle
měření polarizovaných Ramanových spekter



RENISHAW

apply innovation™



At Renishaw, apply innovation is not just a slogan, it's our practice. By applying innovation to every aspect of our design and engineering, we have introduced even more flexibility and more automation for greater ease-of-use; we present InVia Raman microscopes.

out more.



ÚMCH , FZÚ, PŘF UK, ...

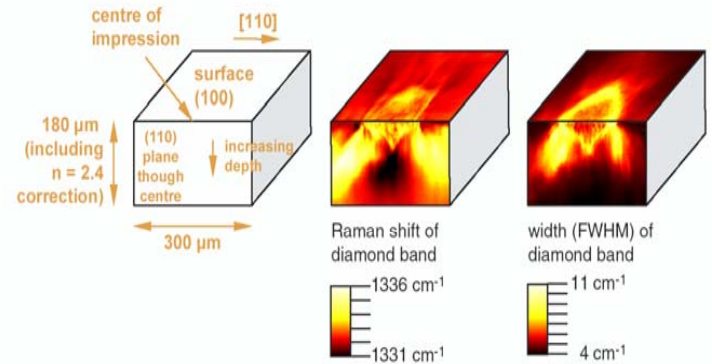
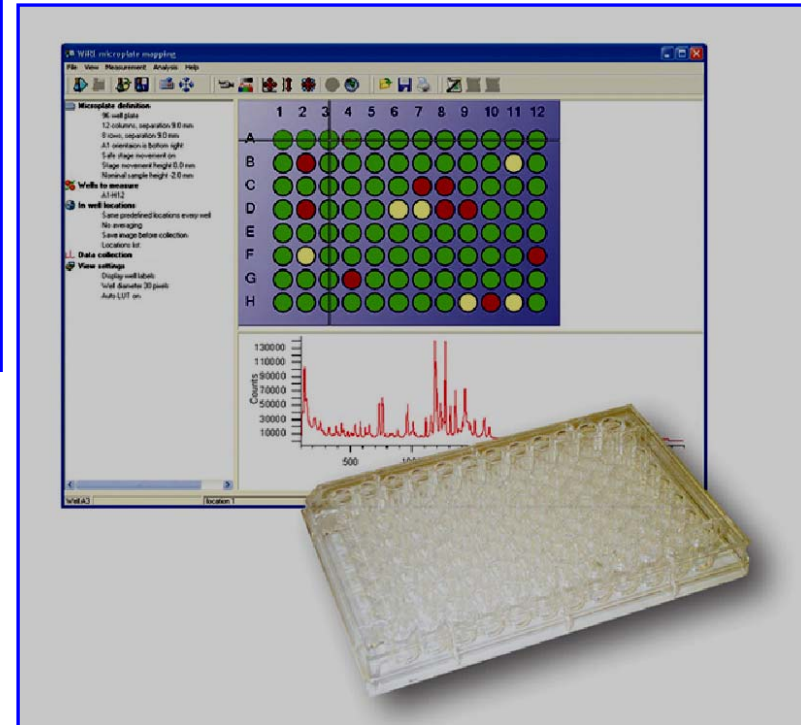
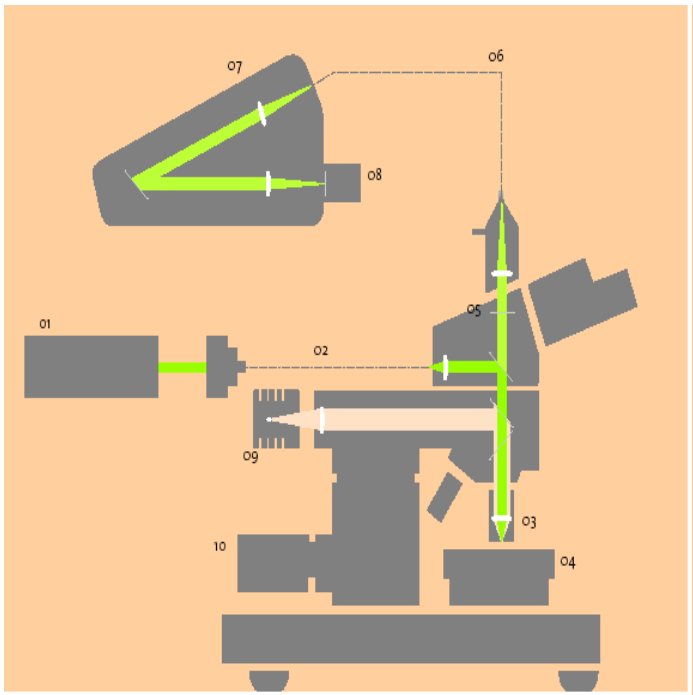
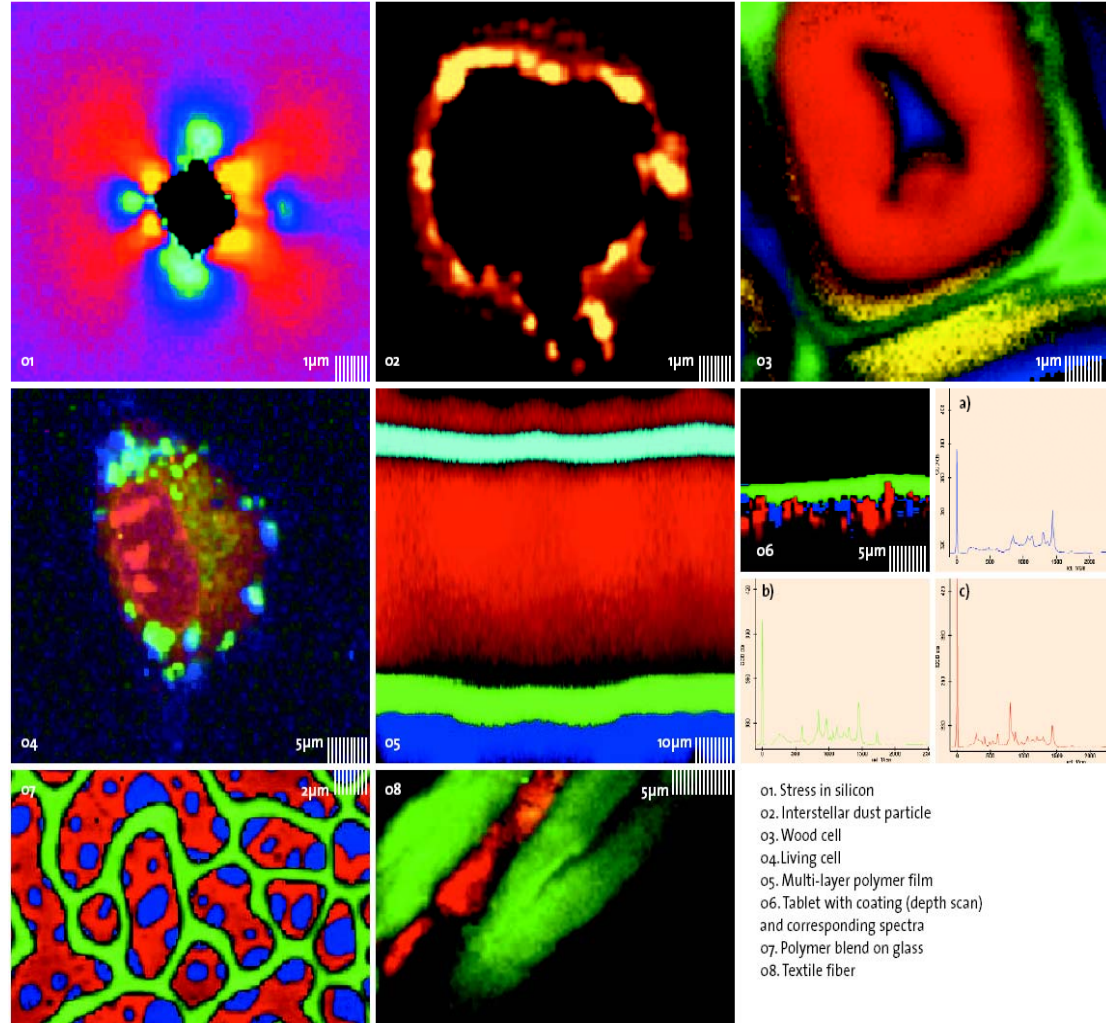


Figure 2
Raman maps of type IIb diamond





- | | |
|-----------------------|----------------------------------------------|
| CRM 200 Beam Path | 06. Multi mode fiber |
| 01. Laser | 07. Lanse based spectroscopy system UHTS 300 |
| 02. Single mode fiber | 08. CCD Detektor |
| 03. Objective | 09. White light illumination |
| 04. Scan table | 10. Z-stage for focusing |
| 05. Filter | |



- 01. Stress in silicon
- 02. Interstellar dust particle
- 03. Wood cell
- 04. Living cell
- 05. Multi-layer polymer film
- 06. Tablet with coating (depth scan) and corresponding spectra
- 07. Polymer blend on glass
- 08. Textile fiber

Kombinace s AFM